Supplementary Materials for

Terahertz Vortices with Tunable Topological Charges from a Laser-Plasma Channel

Linzheng Wang,[a,b] Yanping Chen,[a,b,*] Chen Wang,[a,b] Huanyu Song,[a,b] Jinyu Hua,[a,b] Rongf Huang,[a,b] Min Chen,[a,b] Zhengming Sheng[a,b,c,+]

[a] Shanghai Jiao Tong University, Key Laboratory for Laser and Plasma (MOE), School of Physics and Astronomy, 800 Dongchuan Road, Shanghai, China, 200240

[b] Shanghai Jiao Tong University, Collaborative Innovation Centre of IFSA, 800 Dongchuan Road, Shanghai, China, 200240

[c] Tsung-Dao Lee Institute, 1 Lisuo Road, Shanghai, China, 201210

*****Yanping Chen**,** E-mail: yanping.chen@sjtu.edu.cn

[+]Zhengming Sheng, E-mail: zmsheng@sjtu.edu.cn

1 Injection conditions for the cylindrical spiral laser trajectory inside a plasma channel

In our considered situation, the plasma channel is cylindrically symmetric. As the refractive index [48] $n_p = \sqrt{1-\omega_p^2/\omega^2}$ of the plasma is decided by the plasma density, such a plasma channel have higher refractive index paraxially, thus can guide the laser for long distance propagation. According to the eikonal equation and laser group velocity equation in the cylindrical coordinate, the laser centroid trajectory with incident position (y_0, z_0) and incident angle $\theta_{x,y,z}$ to the coordinate axes can be described by [35]

$$\frac{\mathrm{d}r}{\mathrm{d}x} = \pm\frac{1}{\cos\theta_x}\left(1-\frac{n(r)}{n_c}-\left(1-\frac{n_{e0}}{n_c}\right)\cdot\left(\sin^2\theta_y\frac{b^2}{r^2}+\cos^2\theta_z\right)\right)^{1/2}, \qquad \frac{\mathrm{d}\varphi}{\mathrm{d}x} = \frac{b\sin\theta_x}{r^2\cos\theta_x}, \tag{S1}$$

Here, $r=\sqrt{y^2+z^2}$, n_c is the critical plasma density, n_{e0} is the plasma density at the incident point (y_0, z_0). $\theta_{x,y,z}$ can be linked with the injection direction (θ, φ) in spherical coordinate system through $\cos\theta_x = \cos\theta$, $\cos\theta_y = \sin\theta\cos\varphi$ and $\cos\theta_z = \sin\theta\cos\varphi$. Here, θ is defined as the angle between the injection direction and the *x*-axis. Note that we take the two independent quantities $\theta_{y,z}$ for further analysis, and θ_x can be derived through $\theta_x = \arccos(\sqrt{1-\cos^2\theta_y-\cos^2\theta_z})$. Variable $b = (z_0 - y_0\cos\theta_z/\cos\theta_y)/(\sqrt{(\cos\theta_z/\cos\theta_y)^2+1})$ is the "striking distance", which is defined as the

distance between the projection of the incident laser pulse and the point of the plasma channel center.

From Eq. S1, it is obvious that both the trajectory radius r and the cyclotron speed $\mathrm{d}\varphi/\mathrm{d}r$ changes while propagation, associating with a complex three-dimensional trajectory. Here, we consider the injection condition for a cylindrical spiral around the channel axis as discussed in the main text. In this case, the trajectory radius keeps the same while the position vector (y, z) rotates around the channel axis at a uniform rate. Therefore, the boundary conditions for a cylindrical spiral trajectory can be derived as

$$\begin{aligned} \frac{dr}{d\mathrm{x}} &= 0\,, \\ \frac{d\varphi}{d\mathrm{x}} &= \mathrm{const.} \end{aligned} \tag{S2}$$

Moreover, as the transverse distance of the laser centroid away from the channel center is fixed in a cylindrical spiral, the plasma density at the laser centroid $n = n_{e0}$ remains the same as in the injection position. Substituting Eq. (S2) to Eq. (S1), it can be derived that

$$(z_0 - y_0 \cos\theta_z / \cos\theta_y)/(\sqrt{(\cos\theta_z / \cos\theta_y)^2 + 1}) = \sqrt{{y_0}^2 + {z_0}^2}\,. \tag{S3}$$

Finally, one can obtain the injection condition for cylindrical trajectory as

$$z_0 \cos\theta_z = y_0 \cos\theta_y. \tag{S4}$$

This result indicates that when the off-axis vector is vertical to the injection direction vector, the laser centroid should keep a cylindrical spiral. Note that Eq. (S1) is derived with the paraxial approximation, thus the modulus of the off-axis vector (y_0, z_0) is limited within the beam diameter.

2 Reconstruction of terahertz far-field features

Based on the analysis in the main text, the THz field can finally be derived as

$$d\boldsymbol{E}_{\mathbf{THz}}(x, R, \varphi) \propto \boldsymbol{R_J}(x)\delta\left(\varphi - \frac{z_0 \tan\theta_y}{|z_0 \tan\theta_y|}\frac{2\pi x}{\Lambda_0}\right) \cdot \frac{1}{R} e^{ik_{THz}R} \cdot e^{il\varphi} \tag{S5}$$

where R is the propagation distance to the far field. As shown in Fig. S1, the radiation beamline of the terahertz radiation to the far-field can be derived as

$$r_{far} = \left(x_{far} - x\right) \tan\alpha, \tag{S6}$$

where (x_{far}, r_{far}) is the far-field position and α is the radiation angle. Then, the propagation distance *R* from the radiated position x can be derived as

$$R(x, x_{far}, \alpha) = (x_{far} - x)\sqrt{1 + \tan^2 \alpha}. \quad \text{(S7)}$$

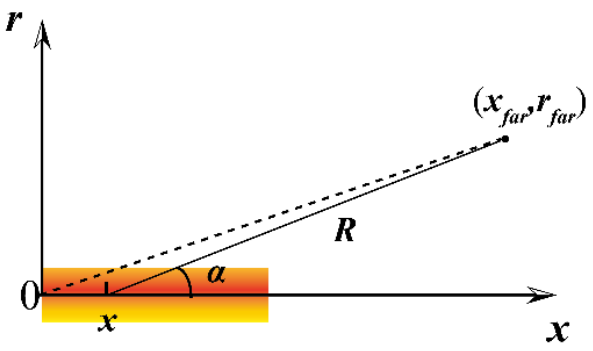

Fig. S1 Schematic about the THz radiation propagation to the far-field.

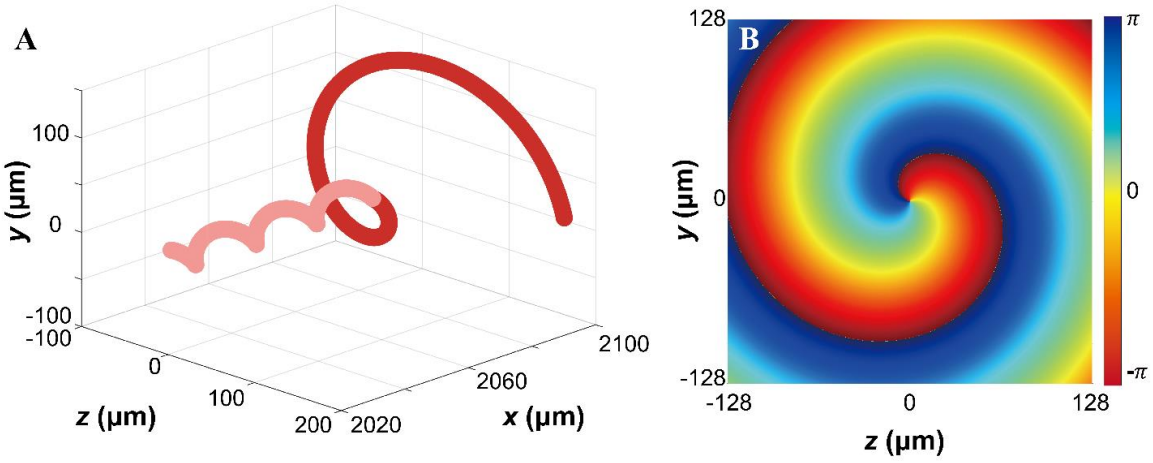

Fig. S2 Reconstruction results of terahertz far-field features. (A) Red line shows the wavefront distribution of the THz radiation. The pink line is the calculated distribution for the following cycles of the THz radiation for the comparison to Fig. 2B. **(B)** The reconstructed phase distribution of the THz radiation at $x_{far} = 2100$ μm.

Based on Eq. (S5) and Eq. (S7), the far-field phase distribution can be reconstructed by calculating the propagation phase as well as the angular phase introduced by the orbital angular momentum carried by the radiation. Moreover, the wavefront structure of the THz radiation in the far-field can be reconstructed by taking the radiation angle α equal to the simulation ones. Taking the injection condition of $z_0 = 10\lambda_0$ and $\theta_y = 88.5°$ as an example, the reconstruction results are given in Fig. S2, in which the reconstruction spatial extent is the same as Figs. 2A and 2B. It is obviously that the calculation results are well-matched with the simulation results.

3 Coordinate transformation and the plasma density setting in 3D PIC simulations

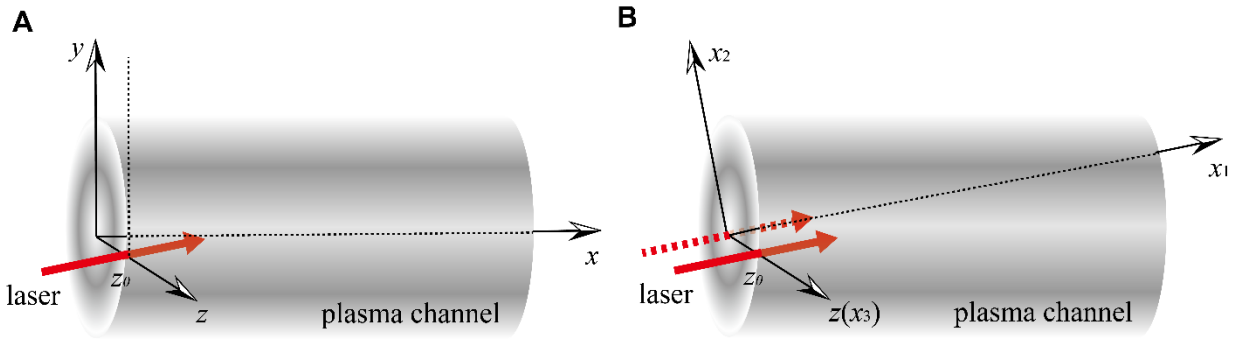

Fig. S3 Coordinate transformation in 3D PIC simulations. (A) shows the plasma channel coordinate. **(B)** is the simulation coordinate utilized in 3D PIC simulations.

In the 3D PIC simulations, we rotate the plasma channel instead of the laser injection axis for convenience as indicated in the Methods part of the main text. Now we give a brief description on the plasma density profile set in our simulations. The initial plasma density profile for a parabolic channel with finite density in the channel coordinate is given by

$$n(r) = \begin{cases} n_0 + \frac{\Delta n r^2}{r_0^2}, & r \le r_c \\ \frac{r_w + r_c - r}{r_w}\left(n_0 + \frac{\Delta n r_c^2}{r_0^2}\right), & r_c < r \le r_c + r_w \end{cases}, \tag{S8}$$

where r_c and r_w are the channel radius and channel wall, respectively. In the Cartesian coordinate system (x, y, z) as shown in Fig. S3A, the plasma density profile is rewritten as

$$n(r) = \begin{cases} n_0 + \Delta n \frac{y^2+z^2}{r_0^2}, & y^2 + z^2 \le r_c^2 \\ (n_0 + \Delta n \frac{r_c^2}{r_0^2}) - \frac{n_0+\Delta n \frac{r_c^2}{r_0^2}}{r_w+r_c}\sqrt{y^2+z^2}, & r_c^2 < y^2 + z^2 \le (r_w + r_c)^2 \end{cases}. \tag{S9}$$

In our simulations, we keep the laser injection axis as the x_1-axis of the simulation box, the direction of the off-axis vector in the injection surface as the x_3-axis, as shown in Fig. S3B. The correspondence between the two coordinate systems can be demonstrated as $x = x_1 \cos\theta_y - x_2 \sin\theta_y$, $y = x_1 \sin\theta_y + x_2 \cos\theta_y$, and $z = x_3$. Substituting these into Eq. (S9), the plasma density profile in the simulation coordinate can be derived as

$$n(r) = \begin{cases} n_0 + \Delta n \frac{x_3^2+(x_1\cos\theta_y - x_2\sin\theta_y)^2}{r_0^2}, & x_3^2 + \left(x_1\cos\theta_y - x_2\sin\theta_y\right)^2 \le r_c^2 \\ (n_0 + \Delta n \frac{r_c^2}{r_0^2}) - \frac{\left(n_0+\Delta n \frac{r_c^2}{r_0^2}\right)\sqrt{x_3^2+(x_1\cos\theta_y - x_2\sin\theta_y)^2}}{r_w+r_c}, & \\ & r_c^2 < x_3^2 + \left(x_1\cos\theta_y - x_2\sin\theta_y\right)^2 \le (r_w + r_c)^2 \end{cases} \tag{S10}$$

Such a plasma density profile is conducted in the 3D PIC simulations within a simulation box moving at the speed of light along the x-direction.

To confine the laser pulse within the simulation box, the laser pulse is initialized around the front rear of the box. The box is set to be asymmetric in the x_2-direction within $280\lambda_0 \le x_2 \le 160\lambda_0$ to investigate the distribution of the terahertz radiation properly. Note that all results given in the main text is already transformed back in the channel coordinate in Fig. S3A.